

Scattering and absorption characteristics of non-spherical cirrus cloud ice crystal particles in terahertz frequency band

Tao Xie(谢涛), Meng-Ting Chen(陈梦婷), Jian Chen(陈健), Feng Lu(陆风), Da-Wei An(安大伟)

Citation: Chin. Phys. B . 2020, 29(7): 074102 . **doi:** 10.1088/1674-1056/ab84d3
Journal homepage: http://cpb.iphy.ac.cn; http://iopscience.iop.org/cpb

What follows is a list of articles you may be interested in

Cherenkov terahertz radiation from Dirac semimetals surface plasmon polaritons excited by an electron beam

Tao Zhao(赵陶), Zhenhua Wu(吴振华)

Chin. Phys. B . 2020, 29(3): 034101 . **doi:** 10.1088/1674-1056/ab6840

New hybrid FDTD algorithm for electromagnetic problem analysis

Xin-Bo He(何欣波), Bing Wei(魏兵), Kai-Hang Fan(范凯航), Yi-Wen Li(李益文), Xiao-Long Wei(魏小龙)

Chin. Phys. B . 2019, 28(7): 074102 . **doi:** 10.1088/1674-1056/28/7/074102

Influence of cutting off position of plasma filament formed by two-color femtosecond laser on terahertz generation

Zhan-Qiang Xue(薛占强), Li-Ping Shang(尚丽平), Hu Deng(邓琥), Qian-Cheng Zhang(张前成), Quan-Cheng Liu(刘泉澄), Wei-Wei Qu(屈薇薇), Zhan-Feng Li(李占锋), Shun-Li Wang(王顺利)

Chin. Phys. B . 2018, 27(5): 054101 . **doi:** 10.1088/1674-1056/27/5/054101

Tunable terahertz radiation from arbitrary profile dielectric grating coated with graphene excited by an electron beam

Zhao Tao, Zhong Ren-Bin, Hu Min, Chen Xiao-Xing, Zhang Ping, Gong Sen, Liu Sheng-Gang

Chin. Phys. B . 2015, 24(9): 094102 . **doi:** 10.1088/1674-1056/24/9/094102

Extraordinary terahertz transmission through subwavelength spindle-like apertures in NbN film

Zheng Xiao-Rui, Cheng Fei, Wu Jing-Bo, Jin Biao-Bing, Zhu Bei-Yi

Chin. Phys. B . 2014, 23(1): 014101 . **doi:** 10.1088/1674-1056/23/1/014101

SPECIAL TOPIC — Terahertz physcis

Scattering and absorption characteristics of non-spherical cirrus cloud ice crystal particles in terahertz frequency band*

Tao Xie(谢涛)[1], Meng-Ting Chen(陈梦婷)[2], Jian Chen(陈健)[1,†], Feng Lu(陆风)[3,‡], and Da-Wei An(安大伟)[3]

[1] School of Remote Sensing and Geomatics Engineering, Nanjing University of Information Science and Technology, Nanjing 210044, China
[2] School of Electronic and Information Engineering, Nanjing University of Information Science and Technology, Nanjing 210044, China
[3] National Satellite Meteorological Centre, China Meteorological Administration, Beijing 100081, China

(Received 22 January 2020; revised manuscript received 2 March 2020; accepted manuscript online 31 March 2020)

We used discrete dipole approximation (DDA) to examine the scattering and absorption characteristics of spherical ice crystal particles. On this basis, we studied the scattering characteristics of spherical ice crystal particles at different frequencies and non-spherical ice crystal particles with different shapes, aspect ratios, and spatial orientations. The results indicate that the DDA and Mie methods yield almost the same results for spherical ice crystal particles, illustrating the superior calculation accuracy of the DDA method. Compared with the millimeter wave band, the terahertz band particles have richer scattering characteristics and can detect ice crystal particles more easily. Different frequencies, shapes, aspect ratios, and spatial orientations have specific effects on the scattering and absorption characteristics of ice crystal particles. The results provide an important theoretical basis for the design of terahertz cloud radars and related cirrus detection methods.

Keywords: scattering characteristics, discrete dipole approximation, terahertz, non-spherical ice crystal particles

PACS: 41.20.Jb, 92.60.Mt, 92.60.Ta, 92.70.Cp **DOI:** 10.1088/1674-1056/ab84d3

1. Introduction

Cirrus clouds are generally distributed from the upper troposphere to the lower stratosphere, covering an average of approximately 20%–30% of the Earth's surface at any given time.[1] By reflecting solar short-wave radiation and absorbing long-wave radiation from the atmosphere and the ground, cirrus clouds play an important role in regulating the radiation budget of the terrestrial gas system. Cirrus clouds are ice clouds, and they are mainly composed of ice crystal particles of various shapes and sizes. When calculating the scattering characteristics of particles, the Mie scattering theory is only applicable to isotropic homogeneous spherical particles. Therefore, the selection of a suitable algorithm to accurately calculate the scattering characteristics of non-spherical ice particles has become a major challenge in the remote sensing of cirrus clouds.

Satellite remote sensing provides an essential means for atmospheric and cloud detection. Passive microwave remote sensing mainly uses millimeter frequency bands that can strongly penetrate cirrus clouds and are primarily used for the remote sensing of temperature, humidity, and precipitation. Typical ice cloud particles, which can be probed by electromagnetic radiation from microwaves to infrared waves, have diameters ranging from 50 μm–400 μm.[2] On the one hand, microwave (0.0003 THz–0.3 THz) satellite remote sensing can penetrate cirrus clouds, but information on clouds containing only large-grained particles is difficult to obtain with microwaves. On the other hand, the near-infrared band (100 THz–400 THz) has a short wavelength, which can obtain information on the upper surfaces of cirrus clouds, but it is difficult to probe the vertical structure of cirrus clouds. The terahertz band has important applications in many research fields.[3–6] The ice cloud particle sizes are within the range of 30 μm–3000 μm wavelengths of the terahertz frequency band (0.1 THz–10 THz).[7] Therefore, the terahertz band is theoretically the best one for simultaneously detecting the horizontal and vertical structure of cirrus clouds.

Many scholars have developed different numerical algorithms that describe the scattering characteristics of non-spherical ice crystal particles. These are the T-matrix method (TMM),[8] finite-difference time-domain (FDTD),[9] and discrete dipole approximation.[10] FDTD is suitable for small particles with complex and heterogeneous shapes. TMM is applicable to all kinds of uniformly symmetric particles, but it has difficulty with numerical stability and convergence.[11] The the discrete dipole approximation (DDA) method has a simple physical concept and is applicable to particles of any shape. Consequently, it has been widely used to calculate the scattering characteristics of non-spherical ice crystal particles. For

*Project supported by the National Natural Science Foundation of China (Grant Nos. 61527805 and 41776181).
†Corresponding author. E-mail: chjnjnu@163.com
‡Corresponding author. E-mail: lufeng@cma.gov.cn
© 2020 Chinese Physical Society and IOP Publishing Ltd

example, Wu *et al.*[12] calculated the attenuation efficiency of several non-spherical ice crystal particles by using the DDA method for millimeter wave cloud radar. They concluded that in actual ice clouds, considering hexagonal ice crystals and elliptical ice crystals as spherical particles of the same volume underestimates their attenuation and backscatter. Ruan *et al.*[13] calculated the radiation characteristics of non-spherical particles according to DDA method, which are different from those calculated for spherical particles of the same volume. Such differences are affected by the shape, scale parameters, and complex refractive indices of the particles. Wang *et al.*[14] used Lorenz–Mie theory and the TMM method to calculate the terahertz scattering characteristics of spherical water droplets and non-spherical ice crystal particles, respectively. The average attenuation of the non-spherical particles was 28 dB/km, which was slightly less than that of the spherical particles at all frequencies. This research shows that the terahertz scattering characteristics of non-spherical particles are of great significance. Despite this, many studies employ only millimeter wave cloud radars, and use of the terahertz frequency band is still very limited. However, the terahertz frequency band is a vital research field for both pure research and its applications.[15–18]

In order to provide a theoretical basis for the detection of non-spherical ice crystals in cirrus clouds, the use of the DDA method to study the scattering characteristics of terahertz non-spherical ice crystal particles is crucial. Therefore, the scattering characteristics of spherical ice crystal particles and water droplets at 94 GHz, 220 GHz, and 340 GHz were calculated using the Mie scattering results as the standard values for the accuracy test. The effects of different frequency bands on spherical ice crystal particles and the effects of particle shape, aspect ratio and orientation on the scattering characteristics of non-spherical ice crystal particles were compared and analyzed.

2. Discrete dipole approximation method

The DDA method is a discrete expression of the integral form of electromagnetic scattering formulas,[19] that is suitable for studying the scattering and absorption characteristics of particles with arbitrary shapes. Its main principle is to assume that a particle can be discretized into N small cubes, and the scattering characteristics of each small cube can be represented by a dipole. Thus, a finite number of discrete, interacting dipole arrays can be used to approximate particles of arbitrary shape. Therefore, the study of the scattering characteristics of actual particles can be transformed into the study of the scattering characteristics of these dipoles.

According to previous studies,[20–23] the DDA method is sufficiently accurate when the following condition is met:

$$|m|kd < 1. \tag{1}$$

Here, m is the complex refractive index of the target material, d is the dipole spacing, and $k = 2\pi/\lambda$, where λ is the incident wavelength of the target particle in the vacuum. When the imaginary part of the complex refractive index is large, the absorption efficiency increases. Therefore, it is necessary to lower the value of the dipole spacing d in order to reduce the error.

The relationship between the actual volume V of the target and the number of dipoles N is

$$V = Nd^3. \tag{2}$$

In addition, the relationship between V and the equivalent radius a_{eff} (the radius corresponding to a sphere with a density of 0.916 cm/m^3[24]) is

$$V = \frac{4\pi}{3}a_{\text{eff}}^3. \tag{3}$$

Combining formulas (2) and (3), the formula for a_{eff} is deduced as follows:

$$\begin{aligned} a_{\text{eff}} &= \left(\frac{3V}{4\pi}\right)^{1/3} = \left(\frac{3Nd^3}{4\pi}\right)^{1/3} \\ &= \frac{1}{|m|\cdot kd}\left(\frac{3Nd^3}{4\pi}\right)^{1/3}\cdot|m|\cdot kd. \end{aligned} \tag{4}$$

Formula (4) can be simplified to

$$\begin{aligned} a_{\text{eff}} &= \frac{\lambda}{|m|\cdot 2\pi}\left(\frac{3N}{4\pi}\right)^{1/3}\cdot|m|kd \\ &= 9.88\frac{\lambda}{|m|}\left(\frac{N}{10^6}\right)^{1/3}\cdot|m|kd. \end{aligned} \tag{5}$$

Since $|m|kd < 1$, the equivalent radius a_{eff} satisfies

$$a_{\text{eff}} < 9.88\frac{\lambda}{|m|}\left(\frac{N}{10^6}\right)^{1/3}. \tag{6}$$

Therefore, the number of dipoles N needs to satisfy

$$N > \frac{4\pi}{3}(a_{\text{eff}}k)^3|m|^3 = 4.189(a_{\text{eff}}k)^3|m|^3. \tag{7}$$

Due to limitations in the computing performance of modern computers, the number of dipoles cannot exceed 10^6. For this paper, the main input parameters are frequency (wavelength), particle equivalent radius, particle shape, and particle orientation. The main simulation outputs of the DDA algorithm are the extinction efficiency Q_{ext} (the ratio of the extinction cross section), the scattering efficiency Q_{sca} (the scattering cross section), the absorption efficiency Q_{abs} (the absorption cross section), and πa_{eff}^2 (the maximum cross-sectional area of the particle).

3. DDA simulation and verification of scattering and absorption characteristics of spherical ice crystal particles

Because measuring the scattering characteristics of ice crystal particles is difficult, it is assumed that the simulated results of Mie scattering are accurate for spherical particles. Therefore, in this paper, Mie scattering and the DDA method are used to simulate spherical ice crystal particles with the same parameters. In order to verify the accuracy of the DDA algorithm, calculations were carried out for three frequency bands: 94 GHz, 220 GHz, and 340 GHz. The complex refractive indices of the non-spherical ice crystal particles for the three frequency bands were $m = 1.782 + 0.003\mathrm{i}$, $m = 1.782 + 0.0049\mathrm{i}$, and $m = 1.781 + 0.007\mathrm{i}$, respectively.[25] The range of effective radii of the spherical ice crystal particles simulated in this paper was 50 μm–1550 μm.

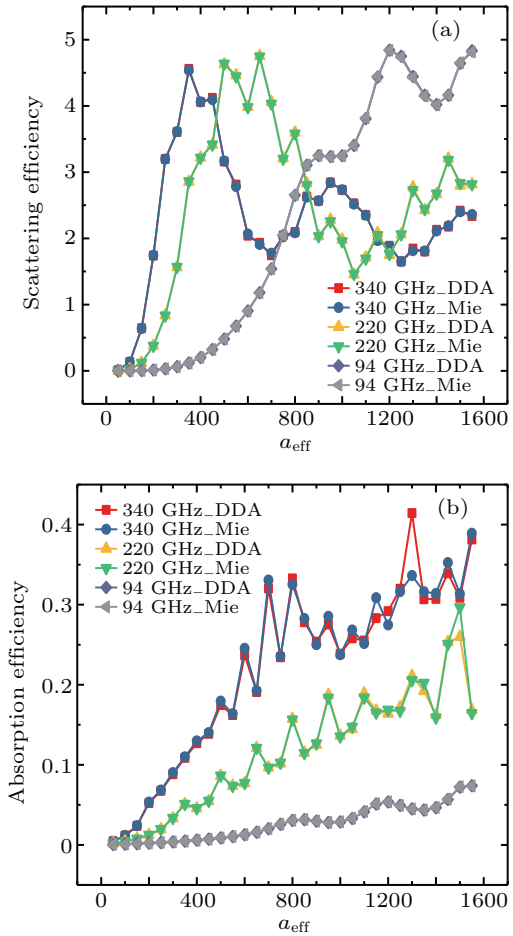


Fig. 1. Scattering and absorption characteristics of ice particles calculated by the DDA and Mie scattering methods.

Based on the DDA and Mie scattering methods, DDSCAT7.3 and MATLAB software were used to calculate the scattering and absorption characteristics of spherical ice crystal particles at 94 GHz, 220 GHz, and 340 GHz. The results are shown in Fig. 1. Figure 1(a) displays the variation in the scattering of spherical ice crystal particles with an equivalent radius in the three bands. They show that the characteristic scattering curves calculated by the DDA and Mie scattering methods are almost identical across the three frequency bands, indicating that the DDA algorithm generated highly accurate scattering characteristics for the non-spherical ice crystal particles. In addition, the equivalent radii of the scattering peaks in the 94-GHz, 220-GHz, and 340-GHz frequency bands are 1200 μm, 500 μm, and 350 μm, respectively. This demonstrates that the terahertz band is more suited to monitor ice crystal particles than millimeter waves.

Figure 1(b) shows the variation of the absorption of spherical ice crystal particles in three frequency bands with equivalent radii. As can be seen from the figure, for 94 GHz and 220 GHz, the absorption curves of spherical ice crystal particles calculated by the DDA and Mie scattering methods are very similar. In the 340-GHz frequency band, the trends of the particle absorption calculated by the two methods are consistent, but there is a vertical offset error, which may be caused by different frequencies or different particle sizes.

In order to compare the two methods more intuitively, we calculated the relative errors between the results generated by the DDA and Mie scattering methods for the scattering of spherical ice crystal particles, as shown in Fig. 2. The figure indicates that the maximum relative errors between the two methods in the 94-GHz, 220-GHz, and 340-GHz bands are 0.41%, 1.50%, and 1.76%, respectively. The absorption relative error of the 220-GHz band is $< 2\%$ within the equivalent radius of 1050 μm; the absorption relative error of the 340-GHz band is $< 3.5\%$ within the equivalent radius of 1100 μm, and the error is $> 3.5\%$ beyond this range. The size of common ice crystal particles is within 1000 μm; therefore, the DDA method is sufficiently accurate in the analysis of the scattering characteristics of non-spherical ice crystal particles.

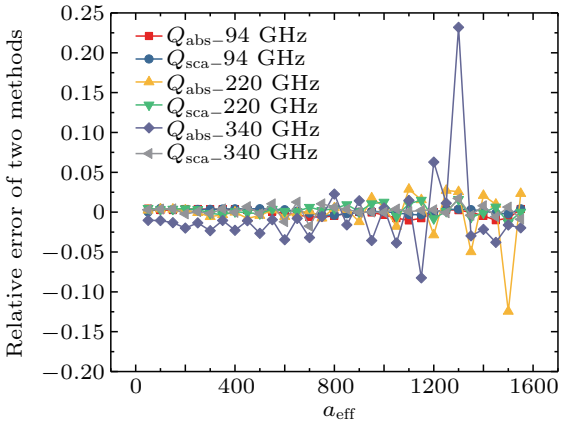


Fig. 2. Relative error of scattering and absorption of two methods.

4. Analysis of scattering and absorption characteristics of non-spherical ice particles

Initially, the ice crystal particles were assumed to be spherical or ellipsoidal, but most of the simulated ice crystal particles were shaped as hexagonal columns, hexagonal

plates, and bullet flowers. Among these, the most common non-spherical particles were hexagonal in shape. Using the aspect ratio, the hexagonal ice crystal particles were divided into the following categories:[26] long column ($L/2a = 4$), thick column ($L/2a = 2$), block column ($L/2a = 1$), thick plate ($L/2a = 1/6$), and thin plate ($L/2a = 1/20$), where L is the height of the hexagonal prism (the distance between the two hexagons at either end of the particle), a is the length of each side of the hexagon, and $2a$ is the distance between the vertical angles of the hexagon. Therefore, the effects of different frequency bands, sizes, aspect ratios, and orientations on the scattering characteristics of hexagonal ice crystal particles could be studied.

4.1. Scattering and absorption characteristics of ice particles in different frequency bands

Figure 3 shows the scattering and absorption characteristics of spherical ice crystal particles with a radius of 600 μm for frequencies lower than 5 THz, as calculated by DDSCAT software. It indicates that the scattering, absorption, and extinction characteristics of spherical particles in different frequency bands exhibit considerable variation. When the frequency is < 1.008 THz, the scattering characteristics show fluctuations with multiple peaks, with the maximum value at 191 GHz, which may be related to the size of ice crystal particles. When the frequency is > 1.008 THz, the extinction efficiency and scattering efficiency of ice crystal particles increase with increasing frequency, while the absorption efficiency decreases. Higher frequencies are more easily absorbed by the ground, causing the absorption efficiency of particles to decrease. According to Li,[27] who studied THz radiation transmission characteristics of the clear sky, the atmospheric window is mainly located near the frequencies of 0.135 THz, 0.23 THz, 0.34 THz, 0.41 THz, 0.67 THz, and 0.87 THz. In addition, since the frequency of 94 GHz is commonly used for cloud and mist detection, the frequency of 220 GHz and 340 GHz are commonly used for ice cloud detection. Therefore, the 220-GHz (1360 μm) and 340-GHz (882 μm) frequency bands were selected for comparison with the 94-GHz (3190 μm) millimeter wave frequency band.

Spherical ice crystal particles and water droplets were selected as representatives in the study of scattering and absorption characteristics at 94 GHz, 220 GHz, and 340 GHz. As shown in Fig. 4, the scattering and absorption characteristics of spherical particles show obvious variation with different frequency bands. Figure 4(a) shows that, in the 340-GHz (terahertz) frequency band, the scattering characteristics of spherical ice crystal particles fluctuate with multiple peaks. Conversely, there is only one peak in the 94-GHz (millimeter) frequency band, which occurs at an equivalent radius of 1200 μm. For the 220-GHz and 340-GHz bands, the first scattering peaks are obtained at equivalent radii of 500 μm and 350 μm, respectively. The positions of the peak scattering efficiencies clearly depend on frequency: the lower the frequency, the larger the corresponding equivalent radius of the scattering peak. The results show that the millimeter wave band is suitable for detecting relatively larger particles and the terahertz frequency band is suitable for detecting smaller particles. Nevertheless, the size of ice crystal particles generally does not exceed 1000 μm; thus, it is more advantageous to use the terahertz frequency band to detect ice crystal particles. As can be seen in Fig. 4(b), the absorption efficiencies of non-spherical particles increase with increasing frequency at all equivalent radii. Therefore, the absorption of particles in the terahertz frequency band is greater than that of the millimeter wave band.

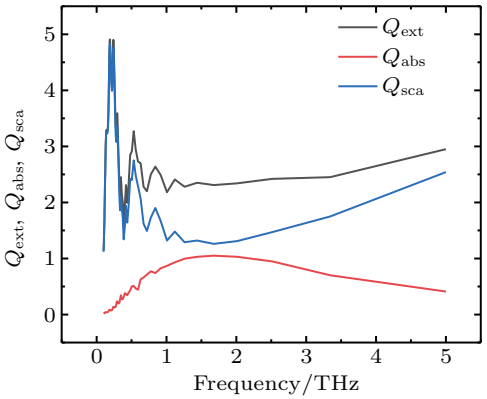


Fig. 3. Scattering, absorption, and extinction characteristics of spherical ice crystal particles with varying frequencies.

Figure 4(a) indicates that the scattering characteristics of water droplets in the 94-GHz, 220-GHz, and 340-GHz bands show a trend of increasing rapidly and then maintaining stability. The scattering peak value in the terahertz band is obtained at relatively small particles, while the scattering peak value in the millimeter wave band is obtained at relatively large particles. In Fig. 4(b), the absorption characteristics of water droplets in terahertz and millimeter wave bands both show a trend of an initial sharp increase followed by gradual decrease. Moreover, the absorption in the terahertz band increases at a faster rate with an approximately vertical ascent, and the absorption peaks in the 94-GHz, 220-GHz, and 340-GHz bands are located at 150 μm, 250 μm, and 500 μm, respectively. A 340-GHz terahertz band scattering curve of spherical ice crystal particles has multiple peaks, while that of water droplets has only one peak, and the scattering peaks of the two respectively occur at 350 μm and 150 μm of small particles. The absorption efficiency of water droplets is obviously higher than that of spherical ice crystal particles (Fig. 4(b)).

To sum up, analyzing the scattering and absorption characteristics of water droplets and ice crystal particles in the 94-GHz, 220-GHz and 340-GHz bands is effective for quantitative remote sensing of ice crystal particles in the terahertz band.

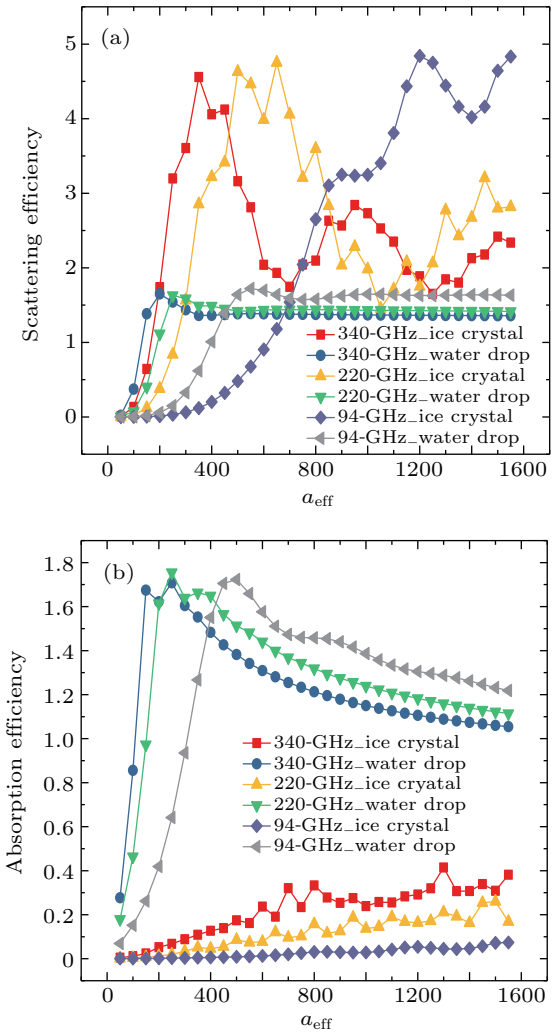


Fig. 4. Scattering and absorption characteristics of ice crystal particles and water drops for different frequency bands.

4.2. Effects of different shapes on scattering and absorption characteristics of ice particles

As shown in Fig. 5, ice crystal particles shaped as block columns, spheres, and ellipsoids were selected as representatives of all the ice particles in order to study the scattering characteristics in the 340-GHz frequency band. Figure 5(a) shows the scattering efficiencies of the three particle shapes as a function of the equivalent radius. This indicates that ice crystal particles of different shapes exhibit different scattering characteristics. The scattering characteristics of the three kinds of particle shapes all exhibit fluctuations with equivalent radii, but the scattering characteristics of the block column particles are not completely consistent with those of the spherical and ellipsoidal particles. The absorption characteristics of the same particles are displayed in Fig. 5(b). This indicates that block column and spherical particles generally show a relatively consistent trend with equivalent radius, but there are still significant differences, especially for larger particle sizes. Conversely, the ellipsoid particles show maximum absorption efficiency at 500 μm, which may be influenced by the particle shape or size.

In summary, the scattering and absorption characteristics of ice crystals are influenced by particles with a wide range of shapes. This suggests that it is unreasonable to assume that particles are either spherical or ellipsoidal and that the exclusion of block column particles introduces additional error.

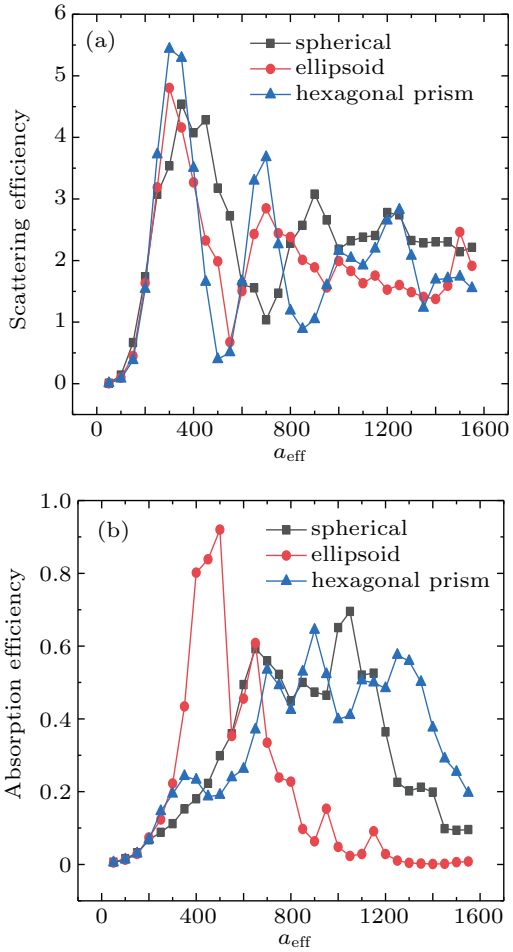


Fig. 5. Effects of different shapes on the scattering and absorption characteristics of ice crystal particles.

4.3. Effects of different aspect ratios on scattering and absorption characteristics of ice particles

Hexagonal ice crystal particles with aspect ratios of $L/2a = 1/20$, $L/2a = 1/6$, $L/2a = 1$, $L/2a = 2$, and $L/2a = 4$ were selected to study the effects of different aspect ratios on particle scattering characteristics in the 340-GHz frequency band, as shown in Fig. 6. The scattering efficiencies of hexagonal particles with different aspect ratios as a function of equivalent radius are displayed in Fig. 6(a). This indicates that the scattering characteristics of hexagonal particles with aspect ratios of 1, 2, and 4 exhibit fluctuations with multiple peaks. Conversely, the scattering curve for particles with an aspect ratio of 1/6 has one maximum value at 5.9778. In addition, the scattering of hexagonal particles with an aspect ratio of 1/20 generally increases with increasing equivalent radius. Within the equivalent radii range of 800 μm–1500 μm, the scattering curve is approximately linear.

Figure 6(b) shows the absorption efficiencies of hexagonal particles with different aspect ratios as a function of equivalent radius. The figure indicates that, on the one hand, the absorption characteristics of particles with aspect ratios of 2 and 4 exhibit fluctuations with multiple peaks. On the other hand, when the aspect ratio is 1, the absorption characteristics of the particles generally show an increase. Furthermore, when the aspect ratio is 1/6, the absorption curve increases until it reaches the maximum value of 0.31848 at 800 μm, then decreases. Finally, when the aspect ratio is 1/20, the absorption efficiency slightly increases initially and then gradually decreases, reaching a maximum value of 0.12558 at 550 μm. Within the equivalent radius range of 600 μm–1550 μm, the trend is approximately linear.

If the aspect ratio is < 1, it is called a hexagonal plate; if it is > 1, it is called a hexagonal column. The above analysis suggests that the scattering characteristics of hexagonal column ice crystal particles show multiple peaks, which are more abundant than those of particles in the shape of a hexagonal plate. In addition, the total absorption value of the hexagonal plate ice crystal particles is smaller than that of the hexagonal column particles. Therefore, ice crystal particles with different aspect ratios have significantly different scattering and absorption characteristics.

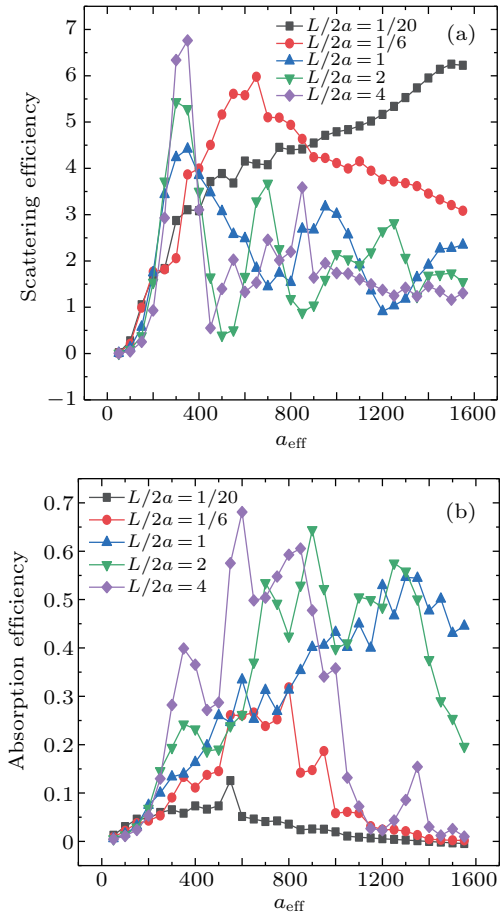


Fig. 6. Effects of different aspect ratios on scattering and absorption characteristics of ice crystal particles.

4.4. Effects of spatial orientation on scattering and absorption characteristics of ice particles

Spatial orientation refers to the position of the particles in space. For non-spherical particles, the spatial orientation of the particles also has significant influence on their scattering characteristics. Laboratory fame (LF) and target fame (TF)[28] were used to determine the spatial orientation of particles. As shown in Fig. 7, the target coordinate system is defined by the longest dimension and second-longest dimension ($\boldsymbol{a}_1$ and $\boldsymbol{a}_2$, respectively) of the target entity.

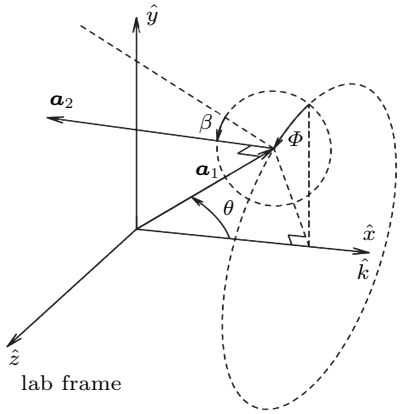


Fig. 7. Target positioning in the laboratory coordinate system.

The orientation of the target in space is determined by the polarization angles θ, Φ, and β, where θ is the angle between $\boldsymbol{a}_1$ and the $\boldsymbol{x}$ axis, Φ is the angle at which $\boldsymbol{a}_1$ rotates about the $\boldsymbol{x}$ axis, and β is the angle at which $\boldsymbol{a}_2$ rotates about $\boldsymbol{a}_1$. In this paper, thick column particles with an aspect ratio of 2 are selected as representatives of all particles. In addition, the following four simple orientations of thick column particles are used: horizontal orientation, oblique orientation 45°, oblique orientation 60°, and vertical orientation. The polarization angles Φ and β corresponding to the four spatial orientations are all identical (*i.e.*, 0), and the polarization angle θ was fixed at values of 0°, 45°, 60°, and 90°.

Figure 8 shows the 340-GHz scattering and absorption characteristics of thick column particles with different spatial orientations. Figure 8(a) depicts the variation in the scattering of particles with different spatial orientations as a function of equivalent radii. The scattering characteristics of the four different spatial orientations all fluctuate with equivalent radii. When $\theta = 0$, the scattering characteristics are very different from the other three all equivalent radii. The maximum value of 7.8319 is reached at the equivalent radius of 350 μm, which may be due to the particle size.

Figure 8(b) depicts the variation in absorption for particles with different spatial orientations as a function of equivalent radii. The absorption characteristics of particles with different spatial orientations show an increasing trend as the equivalent radius increases. When $\theta = 0$, the absorption characteristics show fluctuations with three major peaks, and the

fluctuation range is the largest compared with the other three spatial orientations.

In summary, the variation in spatial orientation of the thick column particles causes significant differences in their scattering and absorption characteristics. This indicates that the wide range of spatial orientations of ice crystal particles introduces uncertainty in cirrus cloud particle detection. However, the results presented in this section indicate that the information obtained by the terahertz frequency band (at 340 GHz) can probe the orientation of cirrus ice crystal particles. Therefore, more research on terahertz cloud radars should be conducted in the future in order to fully exploit this advantage.

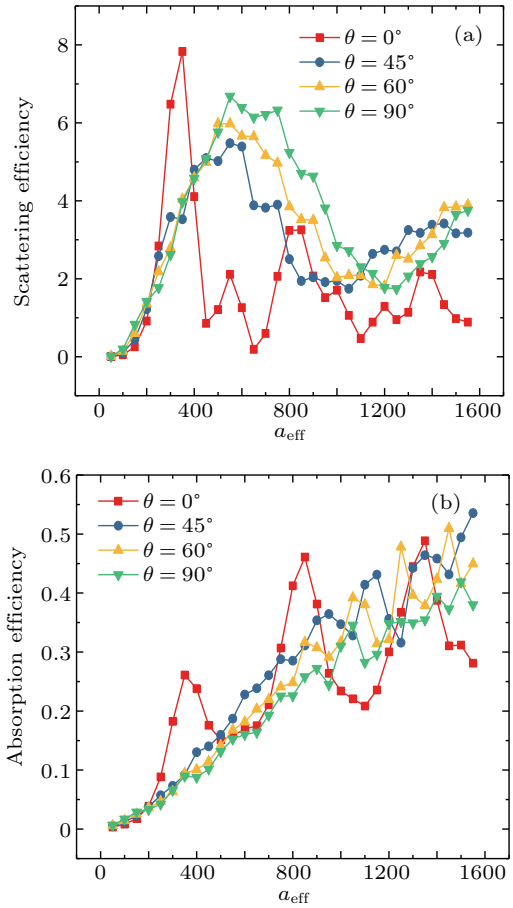


Fig. 8. Effects of different spatial orientations on scattering and absorption characteristics of thick column ice crystal particles at 340 GHz.

5. Conclusions

In this paper, the DDA algorithm was used to study the scattering and absorption characteristics of spherical and non-spherical ice crystal particles with equivalent radii in the range of 50 μm–1550 μm using the terahertz frequency band. The effects of different frequencies, shapes, aspect ratios, and spatial orientations on the scattering and absorption characteristics of cirrus ice crystal particles were analyzed. This provides an important theoretical basis for the design of terahertz cloud radars and the inversion of cirrus parameters. The following are the major results of this paper.

(i) The calculation experiments show that the scattering characteristics of spherical ice crystal particles in DDA and Mie at 94 GHz, 220 GHz, and 340 GHz are almost identical, and the relative error of scattering calculation is $< 1.8\%$. The calculated absorption characteristics of DDA and Mie scattering in 94-GHz, 220-GHz, and 340-GHz bands are highly consistent within the equivalent radius of 1100 μm, and the calculated relative error is $< 3.5\%$. Therefore, the DDA algorithm is suitable for the calculation of scattering and absorption characteristics of non-spherical ice crystal particles.

(ii) The scattering and absorption characteristics of spherical ice crystal particles show different variations in different frequency bands. The millimeter wave band is suitable for monitoring larger particles, but the terahertz band (340 GHz) is more suitable for monitoring the majority of cirrus ice crystal particles because it has a scattering peak at the equivalent radius of 350 μm, which is exactly the size of most ice crystal particles. The scattering of ice crystal particles at 340 GHz is more obvious than that of water droplets, indicating that the terahertz frequency band (340 GHz) is more suitable for remote sensing monitoring of ice crystal particles than the commonly used millimeter wave frequency band (94 GHz).

(iii) A comparison of the scattering characteristics of spherical, ellipsoidal, and hexagonal column particles reveals that the widely used calculation approximation of assuming particles are spherical or ellipsoidal is unreasonable and produces errors when applied to terahertz remote sensing.

(iv) Ice crystal particles with different aspect ratios and different spatial orientations have different scattering and absorption characteristics. In general, the scattering characteristics of hexagonal column particles with horizontal orientation show much more variation than those of hexagonal plate particles, indicating the need for further experimental research.

References

[1] Wang J H, Ge J X, Wei M, Mao B T and Wang J 2013 *S1 Semin. Integr. Meteorological Detect. Tech.*, October 22, 2013, Nanjing, China p. 715
[2] Miloshevich L M and Heymsfield A J 1997 *J. Atmos. Ocean. Technol.* **14** 753
[3] Zhao J W, He M X, Dong L J, Li S X, Liu L Y, Bu S C, Ouyang C M, Wang P F and Sun L L 2019 *Chin. Phys. B* **28** 048703
[4] Wang J, Guo C, Guo W L, Wang L, Shi W Z and Chen X S 2019 *Chin. Phys. B* **28** 046802
[5] Zhang M, Yang Z G, Liu J S, Wang K J, Gong J L and Wang S L 2018 *Chin. Phys. B* **27** 060204
[6] Hu F R, Xu X, Li P, Xu X L and Wang Y E 2017 *Chin. Phys. B* **26** 074219
[7] Liu S G and Zhong R B 2009 *J. Univ. Electron. Sci. Technol. Chin.* **38** 481
[8] Waterman P C 1965 *J. Proc. IEEE* **53** 805
[9] Yang P, Liou K N, Wyser K and Mitchell D 2000 *Geophy. Res.* **105** 4699
[10] Draine B T and Flatau 1994 *Opt. Soc. Am. A* **11** 1491
[11] Xu L S, Chen H B, Ding J L and Xia Z Y 2014 *Adv. Earth Sci.* **29** 903
[12] Wu J X, Wei M, Huang L, Tu H Q and Liu B 2016 *J. Meteorol. Sci.* **36** 63
[13] Ruan L M, Qi H and Wang S G 2008 *J. Harbin Inst. Technol.* **40** 413

[14] Wang Y W, Zhang F, Dong Z W and Sun H F 2016 *IEEE International Conference on Infrared, Millimeter, and Terahertz waves (IRMMW-THz)*
[15] Gu X Y, Wang K J, Yang Z G and Liu J S 2019 *Chin. Phys. B* **28** 098701
[16] Xu D G, Zhu X L, Wang Y Y, Li J N, He Y X, Pang Z B, Cheng H J and Yao J Q 2019 *Chin. Phys. B* **28** 324
[17] Chen A T, Sun H Y, Han Y P, Wang J J and Cui Z W 2019 *Chin. Phys. B* **28** 014201
[18] M Y Y, Huang H C, Hao S B, Tang W C, Zheng Z Y and Zhang Z L 2019 *Chin. Phys. B* **28** 060702
[19] Li X Y, Yang Z L and Zhou H G 2005 *J. Yunnan Univ. (Nat. Sci.)* S1 **150**
[20] Yurkin M A and Hoekstra A G 2007 *J. Quant. Spectrosc. Radiat. Transfer* **106** 558
[21] Draine B T 1988 *Astrophys. J.* **333** 848
[22] Yang W H, Schatz G C and Duyne R P V 1995 *J. Chem. Phys.* **103** 869
[23] Bai J Q 2017 *Discrete Dipole Method to Study Light Scattering Characteristics of Haze Particles* (MS Dissertation) (Xi'an: Xidian University) (in Chinese)
[24] Wu J X, Dou F L, An D W, Chen Q L, Huang L and Tu A Q 2016 *J. Infrared Millim. Terahertz Waves* **35** 377
[25] Shi G Y 2007 *Atmospheric Radiology* (Beijing: Science Press) p. 372 (in Chinese)
[26] Wu J X, Wei M and Zhou J 2015 *Plateau Meteorol.* **33** 252
[27] Li S L, Liu L, Gao T C, Huang W and Hu S 2016 *Acta Phys. Sin.* **65** 100 (in Chinese)
[28] Draine B T and Flatau P J 2010 *User Guide For Discrete Dipole Approximation Code DDSCAT* 7.3